Macromolecules

pubs.acs.org/Macromolecules Article

Copper(II) Chloride/Tris(2-pyridylmethyl)amine-Catalyzed Depolymerization of Poly(*n*-butyl methacrylate)

Michael R. Martinez, Ferdinando De Luca Bossa, Mateusz Olszewski, and Krzysztof Matyjaszewski*

Cite This: *Macromolecules* 2022, 55, 78–87 Read Online

ACCESS | Metrics & More | Article Recommendations | Supporting Information

ABSTRACT: A poly(*n*-butyl methacrylate) macroinitiator with terminal chlorine chain-end functionality (CEF) was depolymerized by ATRP mediated by a copper(II) chloride/tris(2-pyridylmethyl)amine ($CuCl_2$/TPMA) catalyst at 170 °C. Depolymerization reactions with solid loadings between 8 and 21 wt % recovered >40% monomer within 10 min and up to 67% monomer at 8 wt % solid loading. This method was selective to *n*-butyl methacrylate monomer by concurrent depolymerization and distillation on a rotary evaporator. Control experiments confirmed that the reactions stopped due to the loss of CEF before equilibrium was established at the equilibrium monomer concentration. Incubation of the macroinitiators showed evidence of alkyl halide decomposition via lactonization of the chain end, leading to lower initiation efficiencies and an increase in the thermal stability of the polymer.

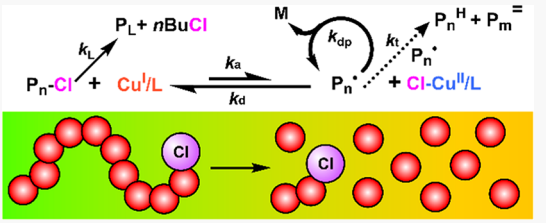

INTRODUCTION

Approximately 45% of the synthetic polymers produced until 2010 were prepared by free radical processes.[1] The majority of these materials are vinyl polymers with aliphatic carbon backbones which are resistant to conventional recycling routes, such as hydrolysis or transesterification. Recent efforts have enabled degradation of vinyl polymers via hydrolysis by statistical incorporation of hydrolyzable groups via radical ring-opening (co)polymerization with heteroatom-containing monomers.[2−4] An alternative approach to vinyl polymer degradation involves depolymerization of polymers back to monomers via a self-immolative approach at elevated temperature.[5,6]

Polymerizations of most vinyl monomers are exothermic and exoentropic, with the enthalpy (ΔH_p) and entropy (ΔS_p) of polymerization being less than zero.[7−9] The positive contribution of the entropic component ($-T\Delta S_p$) increases with temperature, leading to a higher free energy of polymerization and the corresponding increase in the contribution of depropagation for vinyl monomer polymerizations at elevated temperature. Polymerizations of most vinyl monomers are too exothermic for depolymerizations of polymers back to monomers to be feasible because other high activation energy side reactions compete with depropagation at high temperature. The thermodynamics of methacrylic monomers are such that the contribution of depropagation is negligible at room temperature (in most cases) but may become significant at high temperatures or at high dilution when the initial monomer concentration ($[M]_0$) is close to the equilibrium monomer concentration ($[M]_{eq}$).

The impact of depropagation in the high-temperature radical polymerization of *n*-butyl methacrylate (BMA) was extensively studied.[10−16] Conventional radical polymerization of BMA under semibatch conditions plateaued at higher monomer concentrations (i.e., lower conversion) when the temperature was raised from 110 to 145 °C.[11] The effective rate constant of propagation measured by pulsed-laser polymerization (PLP) deviated from the ideal (irreversible) propagation kinetics above a temperature of 120 °C due to an increase in $[M]_{eq}$.[16] The $[M]_{eq}$ of BMA in high-temperature semibatch polymerizations in xylene and pentyl propionate between a temperature range of 110−145 °C followed the scaling relationship $[M]_{eq} = 1.76 \times 10^6(1 - 0.778x_{wp}) \exp(-6240/T)$, where x_{wp} represents the weight fraction of the polymer in the system.[11] Thus, the measured equilibrium monomer concentration of BMA increased with temperature and was higher at high dilution.

Most polymethacrylates can be depolymerized to monomers by pyrolysis above the ceiling temperature (T_c) and thermal degradation temperature (T_d).[17] Thermal degradation of poly(methyl methacrylate) (PMMA) can be initiated by scission of weaker head−head bonds at lower temperature (150−250 °C), degradation of unsaturated end groups at the chain ends at moderate temperature (~300 °C), and random scission at higher temperature (320−450 °C).[18−23] Scission of head−head bonds and unsaturated end groups generate tertiary radicals which can induce depolymerization until the polymer chain is saturated or capped with a more thermally

Received: October 28, 2021
Revised: December 2, 2021
Published: December 22, 2021

https://doi.org/10.1021/acs.macromol.1c02246
Macromolecules 2022, 55, 78−87

stable end group.[24−26] Random chain scission along the backbone was reported to generate one tertiary radical and one primary radical.[27] Both chain ends can lead to depolymerization; however, fragmentation of ester can lead to further decomposition of the side chain into other volatiles and can cap the chain end with an olefin.[27] Pyrolysis of PMMA was reported to reach near-quantitative monomer recovery (95−99%) between 400 and 525 °C.[23,28−30] Pyrolysis at higher temperature led to a larger fraction of gaseous impurities (e.g., CO, CO_2, and olefins).[29]

It should be noted that the experimental setup and the nature of the monomer can significantly affect the selectivity of poly(methacrylate) pyrolysis. More complex reactors are designed to reduce the residence time of the polymer within the reactor to suppress unproductive side reactions. Pyrolysis of PMMA on a simple benchtop microdistillation apparatus (i.e., 400 °C, bulk, 50 mTorr) recovered 53% MMA.[24] Pyrolysis on a filament pyrolysis setup recovered 84% MMA at 450 °C, and the yields of depolymerization on a Curie point pyrolysis−GC setup were 68% at 350 °C and 98% at 480 °C, respectively.[31] The thermal degradation of longer side-chain poly(*n*-alkyl methacrylate)s follow similar thermal degradation mechanisms to PMMA, however with lower selectivity to the monomer due to a higher propensity to decompose along the ester.[32−35] The yield of the monomer was in the order of 90% for poly(alkyl methacrylates) with bulky side chains in a Curie point pyrolysis−GC setup at 480 °C.[31] Flash pyrolysis of PBMA at 650 °C can yield up to 77.5% monomer,[36] and up to 92% BMA can be recovered via pyrolysis in a tube furnace at 400 °C.[37] A compromise between energy efficiency and selectivity to the monomer may plausibly be feasible by activating, and mediating, depolymerization closer to the T_c by a living process.

Reversible deactivation radical polymerization (RDRP) of methacrylic monomers can reach equilibrium at the $[M]_{eq}$; however, radical termination can lead to loss of chain-end functionalities and an eventual plateau in conversion at a dead-end monomer concentration ($[M]_\infty$) higher than the $[M]_{eq}$.[38−42] There were several reports of methacrylic poly(macromonomer) depolymerization to macromonomers mediated by RDRP. Macroinitiators prepared by RDRP were activated by thermal bond scission in a radical addition fragmentation (RAFT) process and by transition metal catalysts in an atom-transfer radical polymerization (ATRP) approach.[41−43] Depolymerizations were proposed to occur due to an imbalance in the rates of propagation and depropagation at $[M]_0 < [M]_{eq}$, leading to a net rate of depropagation larger than the rate of propagation after the activation of the chain ends. A living depolymerization is expected to continue until $[M] = [M]_{eq}$; however, loss of chain-end functionality (CEF) in depolymerization mediated by RDRP may stop the reaction at a $[M]_\infty < [M]_{eq}$ in an analogous dead-end scenario as the forward reaction.[40]

Poly[poly(dimethylsiloxane) methacrylate] (P(PDMSMA)) and poly[(oligoethylene oxide) methacrylate] (P(OEOMA)) with trithiocarbonate CEF were depolymerized by a RAFT process induced by thermal degradation of the chain end from an initial repeat unit concentration ($[P]_0$) of 100 mM to a $[M]_{eq}$ of ∼ 30 mM.[42] RAFT polymerization conducted at $[M]_0$ = 100 mM with otherwise analogous conditions stopped at a comparable $[M]_{eq}$ as the reverse reaction. Depolymerization of poly(polyhedral oligomeric silsesquioxane methacrylate) (P(POSSMA)) was observed when the ATRP of POSSMA reached equilibrium at ∼80% conversion at 60 °C and then depolymerized to ∼60% conversion over 24 h when the flask was transferred to an oil bath at 90 °C due to less favorable thermodynamics at higher temperature.[41] We have recently reported the depolymerization of P(PDMSMA) by ATRP using a copper(II) chloride/tris(2-pyridylmethyl)amine ($CuCl_2$/TPMA) catalyst at 170 °C.[43] Depolymerization at $[P]_0$ = 0.275 M recovered ∼80% macromonomer with reaction times between 10 min and 2 h. The depolymerization rates were accelerated by electron-transfer reactions from excess ligand to the catalyst and the alkyl halide chain end analogous to an activators regenerated by electron transfer (ARGET) mechanism with tertiary amines as the reducing agent (Scheme 1).[44]

Scheme 1. Simplified Mechanism of Depolymerization by ATRP with Activator Regeneration Proposed in Ref 43

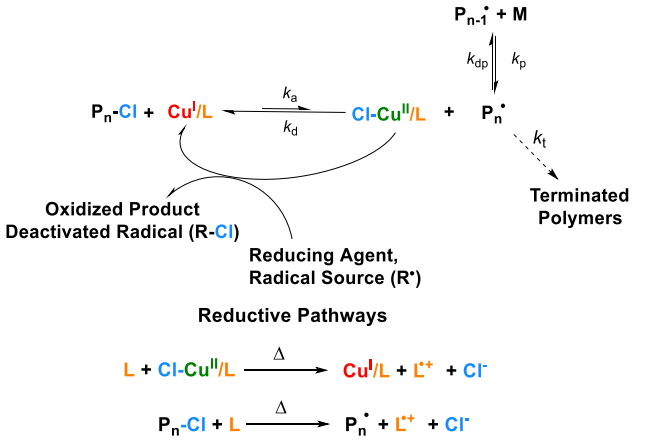

Depolymerizations of less bulky methacrylates are anticipated to be more challenging due to favorable sterics, favoring propagation over depropagation, and significantly higher bulk repeat unit concentrations than macromonomers. This was demonstrated in the depolymerization of less bulky, but industrially relevant, PMMA mediated by an ATRP mechanism with a ruthenium (II) chloride catalyst.[45] Reactions conducted at high dilution (initial polymer concentration ∼10 mM) reached a modest monomer recovery of 8% after 7 h of stirring at 120 °C. Catalyzed depolymerization of methacrylates, which are fast, selective, energy-efficient, and scalable, will require careful optimization of the reaction mechanism and the reactor setup.

In this paper, we investigate the catalyzed depolymerization of PBMA using a copper(II) chloride/tris(2-pyridylmethyl)-amine ($CuCl_2$/TPMA) catalyst in a standard batch setup. Poly(*n*-butyl methacrylate) (PBMA) is commonly used in industrial resins, adhesives, and coatings. Depolymerization under optimized conditions recovered >40% monomer, and up to 67% at higher dilution ($[P]_0$ = 0.75 M, 8 wt % solids), in 10 min. The depolymerization reactions stopped at dead-end monomer concentrations below the $[M]_{eq}$ predicted by the theory. Investigation of chain-end degradation in model experiments confirmed extensive loss of alkyl halide functionality occurred after incubation at 170 °C.

RESULTS AND DISCUSSION

Catalyzed Depolymerization of PBMA. The poly(*n*-butyl methacrylate) macroinitiator was prepared by ARGET

https://doi.org/10.1021/acs.macromol.1c02246
Macromolecules 2022, 55, 78−87

Table 1. Catalyzed Depolymerization of Poly(*n*-butyl methacrylate) by ATRP at 170 °C[a]

experiment	[PBMA−Cl]/[$CuCl_2$]/[TPMA]	$[P]_0$ (M)[b]	x_{wp0}[c]	$[M]_{eq,th}$ (M)[d]	f_t [time, min][e]	$[M]_f$ (M)[f]
L_0	1/0/0	0.75	0.08	1.26	0.001, [120]	0.001
$L_{0.108}$	1/0/0.108	0.75	0.08	1.26	0.28, [120]	0.21
$L_{0.54}$	1/0/0.54	0.75	0.08	1.26	0.41, [120]	0.31
$L_{1.08}$	1/0/1.08	0.75	0.08	1.26	0.55, [120]	0.41
$C_{0.22}L_{1.08}$	1/0.22/1.3	0.75	0.08	1.26	0.67, [30]	0.5
$C_{0.42}L_{1.08}$	1/0.42/1.5	0.75	0.08	1.26	0.65, [30]	0.49
$C_{0.42}L_{1.08}$-1 M	1/0.42/1.5	1	0.11	1.23	0.61, [30]	0.61
$C_{0.42}L_{1.08}$-1.5 M	1/0.42/1.5	1.5	0.17	1.17	0.47, [30]	0.714
$C_{0.42}L_{1.08}$-1.8 M	1/0.42/1.5	1.8	0.21	1.12	0.40, [30]	0.716

[a]Solvent = 1,2,4-trichlorobenzene. [b]Initial repeat unit concentration of the macroinitiator. [c]Initial weight fraction of the polymer. [d]Theoretical extrapolated $[M]_{eq}$ using Hutchinson's scaling from Ind. Eng. Chem. Res., vol. 48, no. 10, 2009—$[M]_{eq} = [1.76 \times 10^6 - 1.37 \times 10^6(x_{p0})] \exp(-6240/T)$ relative to the initial weight fraction of PBMA.[11] [e]Final mole fraction of vinyl functional groups recovered by ^{1}H NMR. [f]Molar concentration of the recovered monomer.

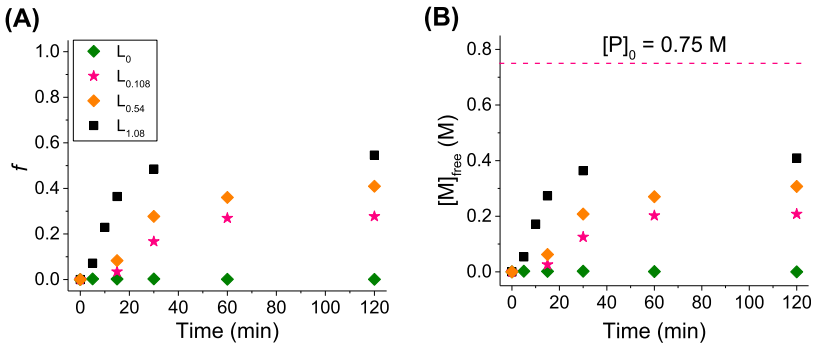

Figure 1. Results of depolymerization of PBMA−Cl at $[P]_0$ = 750 mM in the absence of $CuCl_2$ with different loadings of TPMA. (A) Conversion vs time and (B) $[M]_{free}$ vs time. All reactions were conducted in 1,2,4-trichlorobenzene at 170 °C.

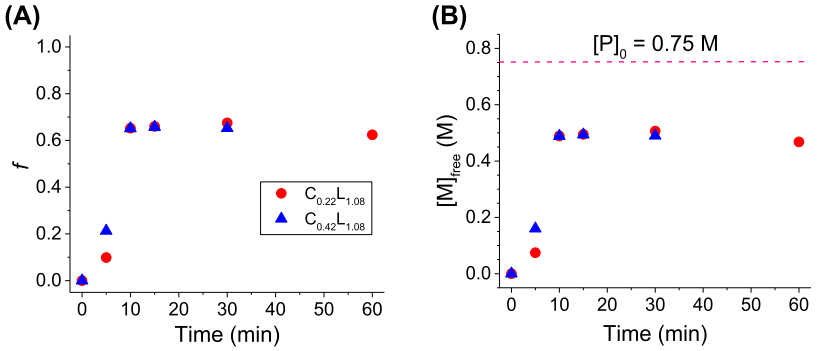

Figure 2. Results of depolymerization of PBMA−Cl at $[P]_0$ = 750 mM with different loadings of $CuCl_2$/TPMA catalyst and 1.08 equivalents of excess TPMA. (A) Conversion vs time and (B) $[M]_{free}$ vs time. All reactions were conducted in 1,2,4-trichlorobenzene at 170 °C.

ATRP with a $CuCl_2$/PMDETA catalyst, an ethyl chlorophenyl acetate (EClPA) initiator, and a $Sn(EH)_2$ reducing agent. Polymerization was performed using a mixture of [BMA]/[EClPA]/[$CuCl_2$]/[PMDETA]/[$Sn(EH)_2$] = [60]/[1]/[0.1]/[0.15]/[0.05] in acetonitrile (30 v/v %) at 70 °C, providing a PBMA−Cl macroinitiator with $M_{n,GPC}$ = 8750 and $Đ$ = 1.17. Polymerization was conducted using a low loading of lower activity $CuCl_2$/PMDETA to increase the rate of ARGET ATRP while maintaining livingness. The chlorine halogen was selected over bromine and iodine due to an anticipated higher thermal stability of the chlorine halogen CEF. ^{1}H NMR of the purified polymer confirmed a DP = 57 by integration of the O−CH_2 protons in the side chains relative to the phenyl protons at the end group (Figure S2).

Catalyzed depolymerization reactions were conducted at 170 °C in 1,2,4-trichlorobenzene with varied concentrations of the $CuCl_2$/TPMA catalyst and excess TPMA ligand (Table 1). The boiling points of the TPMA ligand and solvent are significantly higher than the depolymerization temperature. The reactions are denoted in the format L_XC_Y-P, where X refers to the molar equivalent of the excess TPMA ligand to alkyl halide and Y refers to the molar equivalent of the $CuCl_2$/TPMA catalyst. P is the repeat unit concentration explicitly stated for depolymerization at $[P]_0$ > 0.75 M.

Depolymerization of PBMA−Cl was attempted at low $[P]_0$ = 0.750 M (8 wt % solid content) at 170 °C. Aliquots were removed via a nitrogen-sparged syringe and quenched with air at time points to generate kinetic plots of the vinyl proton mole fraction and monomer concentration via ^{1}H NMR of the crude reaction mixture (Figures 1 and S4). Uncatalyzed depolymerization in the absence of other reagents was negligible after 2 h (L_0, Table 1). The addition of 0.108

https://doi.org/10.1021/acs.macromol.1c02246
Macromolecules 2022, 55, 78−87

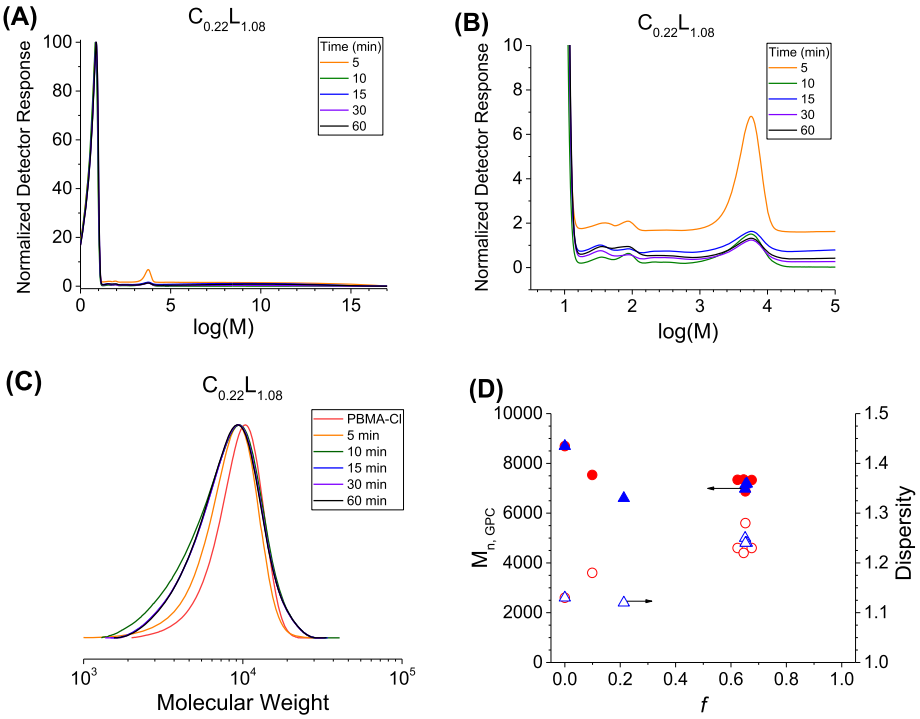

Figure 3. (A) Full normalized GPC traces for each kinetic point in experiment $C_{0.22}L_{1.08}$. The traces are all normalized and calibrated to the 1,2,4-trichlorobenzene peak as the internal standard, with the molecular weight scale relative to the linear PMMA standards in THF. (B) Zoom-in view of GPC traces for experiment $C_{0.22}L_{1.08}$ cutoff to 10% the height of the normalized traces within the range of $M_n = 10^{0.45}$–10^5. (C) Overlaid GPC traces of the high molecular weight fraction in experiment $C_{0.22}L_{1.08}$ normalized to the same height. (D) Molecular weight and dispersity vs f plot for experiments $C_{0.22}L_{1.08}$ (red circle) and $C_{0.42}L_{1.08}$ (blue triangle). The closed symbols correspond to the molecular weight, and the open symbols indicate the dispersity. Both measurements are relative to the linear PMMA standards in THF. The full GPC traces and the GPC traces of the recorded molecular weights and dispersity values for experiment $C_{0.42}L_{1.08}$ are provided in the Supporting Information.

equiv of TPMA in experiment $L_{0.108}$ led to a slow depolymerization plateauing at $f = 0.28$ (Figure 1). Increasing the concentration of TPMA by a factor of 5 led to $f = 0.41$ in experiment $L_{0.54}$. A molar excess of ligand relative to alkyl halide, at 1.08 equiv of TPMA, increased the rate of depolymerization appreciably. This led to a more efficient depolymerization which reached $f = 0.55$ and a corresponding final monomer concentration of $[M]_f = 0.409$ M in 2 h ($L_{1.08}$, Table 1 and Figure 1). These results confirmed an increase in the rate of depolymerization with the concentration of free ligand in the absence of the complete $CuCl_2$/TPMA catalyst, which may be attributed to the reduction of the chlorine chain end leading to activation, and subsequent unzipping, of the macroinitiator.

Catalyzed depolymerization was attempted with 0.22 equiv of the $CuCl_2$/TPMA catalyst while maintaining the same 1.08 equiv of uncoordinated TPMA. The rate of depolymerization significantly accelerated with the complete catalyst (Figure 2). Depolymerization $C_{0.22}L_{1.08}$ recovered ~10% monomer in the first 5 min and plateaued at $f = 0.67$ in 10 min ($C_{0.22}L_{1.08}$, Table 1). No further increase in monomer concentration was observed after stirring the reaction for 1 h (Figure 2). Further increasing the $CuCl_2$/TPMA concentration to 0.42 equiv increased the rate of depolymerization at the early stage, reaching $f \sim 0.2$ in 5 min but reached comparable $f = 0.67$ as $C_{0.22}L_{1.08}$ in 10 min.

The molecular weight of the crude products from experiments $C_{0.22}L_{1.08}$ and $C_{0.42}L_{1.08}$ was recorded at each time point by THF GPC (Figure 3). The full GPC traces were calibrated using linear PMMA standards with the 1,2,4-trichlorobenzene peak as the internal standard and flow marker (Figure 3A). The zoomed-in spectra cut off at 10% of the height of the solvent peak show the full molecular weight distribution of the products at each kinetic point for experiment $C_{0.22}L_{1.08}$ (Figure 3B, data for $C_{0.42}L_{1.08}$ is provided in the Supporting Information). The molecular weight of the high molecular weight fraction above $M_{n,GPC} = 1000$ closely matches that of the original macroinitiator, despite the increase in depolymerization yield and the decrease in polymer peak intensity. Notably, the low molecular weight fraction below $M_{n,GPC} = 100$ does not change significantly despite the increase from $[M] = 0.075$ M at $t = 5$ min to the plateau at $[M] = 0.49$ M at $t = 10$ min. This suggests that the depolymerization was near quantitative for all chains which were activated; however, the monomer and plausible short oligomers and unimer impurities are likely covered by the solvent peak.

Overlaying the high molecular weight fraction in the GPC traces showed a shift toward lower molecular weight, with most of the shift appearing as low molecular weight tailing (Figure 3C). The high molecular weight fraction of PBMA in depolymerization experiments $C_{0.22}L_{1.08}$ and $C_{0.42}L_{1.08}$ decreased starting from $M_{n,GPC} = 8750$ to lower $M_{n,GPC} = 7350$ and $M_{n,GPC} = 7150$, respectively. The $M_{n,GPC}$ value of both experiments decreased with f until $f \sim 0.2$ (Figure 3D). The plateau in molecular weight may be attributed to the accumulation of chains lacking CEF from radical termination during the synthesis of the polymer macroinitiator, leading to lower initiation efficiency, and accumulation of chains lacking alkyl halide functionality due to termination or chain-end degradation during the depolymerization process. Unlike

https://doi.org/10.1021/acs.macromol.1c02246
Macromolecules 2022, 55, 78−87

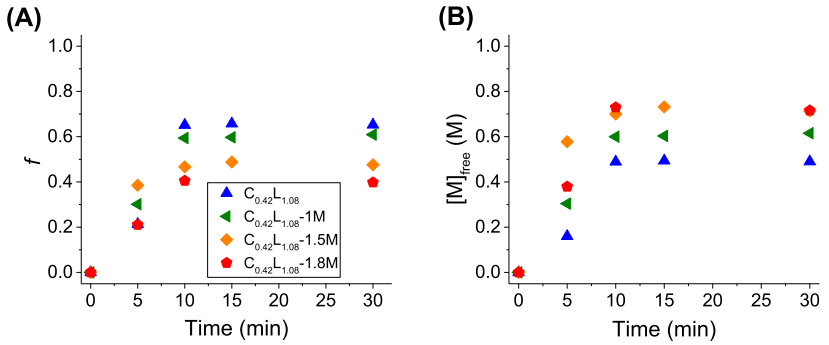

Figure 4. Results of depolymerization of PBMA−Cl using the same [PBMA−Cl]/[$CuCl_2$]/[TPMA] = 1/0.42/1.5 mixture scaled to $[P]_0$ = 0.75−1.8 M. (A) Conversion vs time and (B) $[M]_{free}$ vs time plots. All reactions were conducted in 1,2,4-trichlorobenzene at 170 °C.

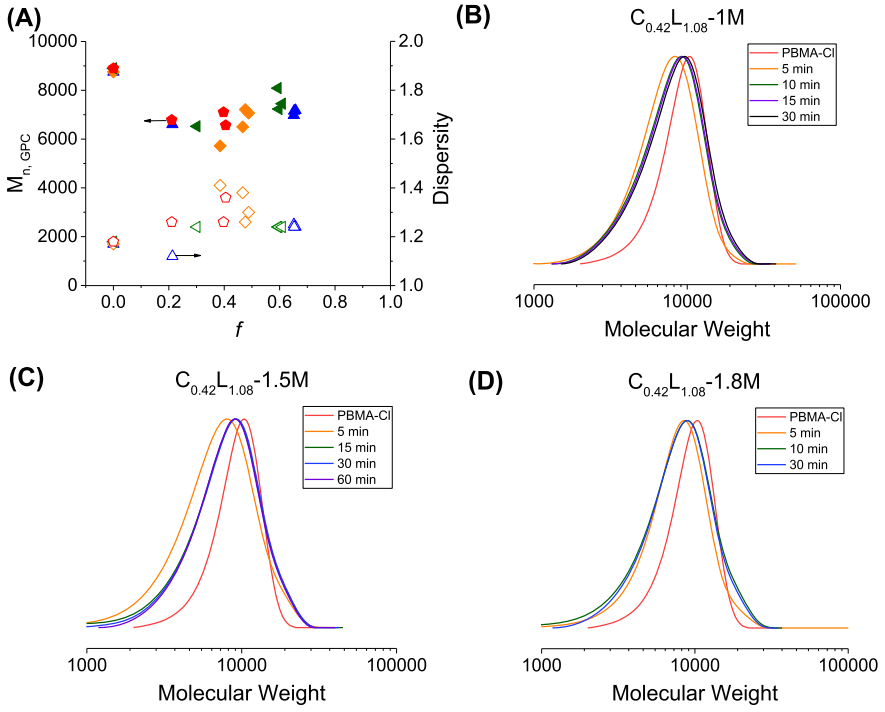

Figure 5. (A) Molecular weight (closed symbols) and dispersity (open symbols) vs f plots for depolymerization at different $[P]_0$ with the mixture [PBMA−Cl]/[$CuCl_2$]/[TPMA] = 1/0.42/1.5. The molecular weight and dispersity are for the high molecular weight fraction with M_n > 1000. $C_{0.42}L_{1.08}$ = blue triangles, $C_{0.42}L_{1.08}$-1 M = green triangles, $C_{0.42}L_{1.08}$-1.5 M = orange diamonds, and $C_{0.42}L_{1.08}$-1.8 M = red pentagons. (B) Overlaid GPC traces of the high molecular weight fraction in experiment $C_{0.42}L_{1.08}$-1 M normalized to the same height. (C) Overlaid GPC traces of the high molecular weight fraction in experiment $C_{0.42}L_{1.08}$-1.5 M normalized to the same height. (D) Overlaid GPC traces of the high molecular weight fraction in experiment $C_{0.42}L_{1.08}$-1.8 M normalized to the same height. The molecular weight and dispersity of the polymers are relative to the linear PMMA standards in THF. The full and zoomed-in views of the GPC traces of all experiments are provided in the Supporting Information.

depolymerization via pyrolysis, the catalyzed depolymerizations at 170 °C can only activate polymers with halogen CEF and other terminated chains are kinetically trapped. The dispersity of the macroinitiator increased after depolymerization, in agreement with what was observed in the catalyzed depolymerization of P(POSSMA) by ATRP.[41]

Depolymerization reactions were conducted at various concentrations using the mixture [PBMA−Cl]/[$CuCl_2$]/[TPMA] = 1/0.42/1.5, with the catalyst and ligand concentrations scaled to $[P]_0$ (Table 1). Increasing the repeat unit concentration led to faster depolymerization, which liberated a lower fraction of the monomer but higher molar concentrations of the monomer (Figure 4). The increase in the rate of depolymerization may be attributed to an increase in the concentration of alkyl halide, catalyst, and reducing agent (excess TPMA), which will increase the radical concentration. Thus, the decrease in the fraction of polymer depolymerized may be attributed to both a higher rate of termination and a lower $[M]_{eq}$, as measured by PLP experiments at varied x_{wp}.[11] Experiment $C_{0.42}L_{1.08}$-1 M ($[P]_0$ = 1 M) depolymerized faster than experiment $C_{0.42}L_{1.08}$ ($[P]_0$ = 0.75 M), reaching higher [M] = 0.61 and lower f = 0.61 in 10 min (Figure 4). $C_{0.42}L_{1.08}$-1.5 M ($[P]_0$ = 1.5 M) and $C_{0.42}L_{1.08}$-1.8 M ($[P]_0$ = 1.8 M) experiments both stopped at [M] = 0.715 M, with different f = 0.47 and 0.40, respectively.

Depolymerization reactions under more concentrated conditions showed a general decrease in molecular weight with conversion (Figure 5A). Interestingly, the high molecular weight fraction of $C_{0.42}L_{1.08}$-1 M shifted to its lowest molecular weight of $M_{n,GPC}$ = 6520 ($Đ$ = 1.24) within the first 5 min (f =

https://doi.org/10.1021/acs.macromol.1c02246
Macromolecules 2022, 55, 78−87

Table 2. Chain Equilibration Experiments at 170 °C[a]

experiment	[BMA]/[PBMA−Cl]/[$CuCl_2$]/[TPMA]	$[M]_0$ (M)[b]	$[P]_0$ (M)[c]	f_0[d]	f_f [time, min][e]	$[M]_f$ (M)[f]
E1	175/1/0.42/1.5	0.5	0.75	0.66	0.92, [120]	0.69
E2	175/1/0.42/1.5	0.716	0.95	0.75	0.89, [120]	0.842

[a]Solvent = 1,2,4-trichlorobenzene. [b]Initial monomer concentration. [c]Initial repeat unit concentration of the macroinitiator and monomer. [d]Initial mole fraction of vinyl functional groups measured by ^{1}H NMR. [e]Final mole fraction of vinyl functional groups measured by ^{1}H NMR. [f]Monomer concentration after 2 h.

0.3) (Figure 5B). The molecular weight plateaued at a higher $M_{n,GPC}$ of ∼ 7,000 ($Đ$ ∼ 1.24) once f = 0.61 and the reaction stopped. A similar trend was observed in experiment $C_{0.42}L_{1.08}$-1.5 M. The high molecular weight fraction decreased starting from $M_{n,GPC}$ = 8750 ($Đ$ = 1.17) to $M_{n,GPC}$ = 5720 ($Đ$ = 1.41) at f = 0.39 in the first 5 min (Figure 5C). The reaction plateaued at a final f = 0.47 and a higher $M_{n,GPC}$ of ∼ 7,000 with a lower $Đ$. The full GPC traces of both experiments showed a decrease in peak intensity after 5 min, in agreement with further depolymerization observed in the ^{1}H NMR spectra (Figures S5 and S6). We believe that this increase in molecular weight at high f may be attributed to a decrease in the weight fraction of chains with CEF, such that the fraction of kinetically trapped dead chains outnumbers the remaining chains with chlorine CEF. The chains lacking CEF closely match the molecular weight of the macroinitiator and are unable to depolymerize. It should be noted that the initiation efficiency of PBMA−Cl was not quantitative, so a significant fraction of the macroinitiator will not be available for depolymerization and a portion of the dead polymer will have a comparable molecular weight to the macroinitiator. The effects of dead-chain accumulation and molecular weight distributions during depolymerization are being investigated in detail as part of the future work.

No depolymerization reactions were able to reach the predicted $[M]_{eq}$ based on the theory. Depolymerization reactions at $[P]_0 < [M]_{eq}$ are predicted to reach quantitative conversion in the absence of radical termination and decomposition of the alkyl halide chain end, neglecting the differences in thermodynamics at short chain lengths. A chain equilibration experiment was conducted with $[M]_0$ = 0.5 M BMA monomer and 0.25 M PBMA−Cl macroinitiator, at, f_0 = 66% and $[P]_0$ = 0.75 M, to confirm whether the depolymerization reaction at $[P]_0$ = 0.75 M stopped due to the loss of CEF or if $[M]_f = [M]_{eq}$ under these conditions (E1, Table 2). In an ideal living polymerization, a macroinitiator initiated at $[M]_0 = [M]_{eq}$ should exchange monomer with no increase in monomer yield or monomer conversion to polymer because the reaction is at equilibrium. The macroinitiator can still depolymerize if $[M]_0 < [M]_{eq}$. Chain equilibration experiment E1 slowly depolymerized to $[M]_f$ = 0.69 M in 2 h, corresponding to an increase in f from 66 to 92% (Figure 6). Equilibration experiment E2 was conducted at $[M]_0$ = 0.715 M and f_0 = 0.75 also led to depolymerization, confirming that the plateau in experiments $C_{0.42}L_{1.08}$-1.5 M and $C_{0.42}L_{1.08}$-1.8 M was likely due to kinetic rather than thermodynamic reasons.

We hypothesized that continuous monomer removal via distillation would improve monomer recovery by consistently displacing the monomer before equilibrium is established at the $[M]_{eq}$ and increasing the overall apparent rate of depolymerization by slowing propagation (i.e., $R_{dp,app} = k_{dp}[P^*] - k_p[M][P^*]$). Depolymerizations were conducted in higher boiling point BMIMTFSI ionic liquid and diethyl phthalate solvents using the optimized [PBMA−Cl]/[$CuCl_2$]/[TPMA] = 1/0.42/1.5 mixture, at $[P]_0$ = 1 M and T = 170 °C,

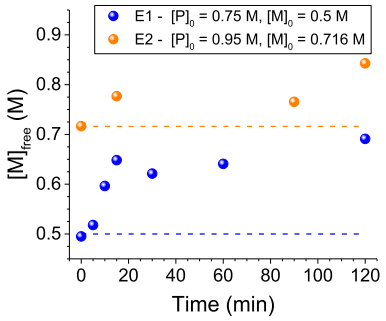

Figure 6. Concentration of monomer in chain equilibration experiments E1 and E2. The experiments were conducted using the mixture [BMA]/[PBMA−Cl]/[$CuCl_2$]/[TPMA] = 175/1/0.42/1.5 with stated $[M]_0$ and $[P]_0$ at 170 °C in 1,2,4-trichlorobenzene. The dotted lines mark the initial $[M]_0$ concentration in the equilibration experiments.

on a Buchi R-215 rotary evaporator (Table 3). The ionic liquid was anticipated to have a lower rate constant of termination relative to the other solvents in this study;[46] however, the PBMA−Cl macroinitiator was insoluble in BMIMTFSI (Figure S8). The flask was loaded onto the rotary evaporator and degassed at a pressure of 56 mbar with a rotation rate of 140 rpm for 60 min before it was lowered into an oil bath preheated to 170 °C at the same pressure and rate of stirring. The flask started to boil three min after being lowered into the oil bath. The volatiles condensed in the bump trap of the apparatus, with no visible droplets in the receiving flask. The distillates condensed in the bump trap consisted of the BMA monomer and a trace of DMF (used to load the $CuCl_2$ catalyst as a stock solution) (Figures S9 and S10). The molecular weight of the macroinitiator decreased from $M_{n,GPC}$ = 8750 to 7646 and the dispersity increased from 1.17 to 1.19 after depolymerization on the rotary evaporator.

Depolymerization in diethyl phthalate was homogeneous (Figure S11), which enabled calculation of f and the fraction of the distilled monomer (v) (Figure S12). 41% of the macroinitiator was degraded to a monomer over the 1 h reaction. The majority of the BMA monomer was condensed in the bump trap (v (%) = 36) along with DMF used to add the $CuCl_2$ salt as a stock solution (Figure S13). Notably, both depolymerization reactions were less efficient at monomer recovery than the $C_{0.42}L_{1.08}$-1 M experiment conducted in 1,2,4-trichlorobenzene under batch conditions with otherwise identical conditions. The lower recovery may be due to inefficient monomer removal or differences in kinetics between solvents.

In all cases, catalyzed depolymerizations with the complete catalyst reached appreciable depolymerization yields (>40% conversion to monomer) within 10 min. However, they were still stopping below the theoretical $[M]_{eq}$ which should be achievable in an ideal living process. Depolymerizations of PBMA by RDRP provided less monomer than pyrolysis

https://doi.org/10.1021/acs.macromol.1c02246
Macromolecules 2022, 55, 78−87

Table 3. Depolymerization Conducted on a Buchi Rotary Evaporator[a]

experiment	solvent	homogeneous?	f (%)[b]	v (%)[c]	pressure (mbar)	$M_{n,GPC}$[d]	$Đ$[d]
vac1	BMIMTFSI	no	n.d.	n.d.	56	7646	1.19
vac2	diethyl phthalate	yes	41	36	70	7438	1.25

[a]Molecular weight of the starting PBMA−Cl macroinitiator $M_{n,GPC}$ = 8750 and dispersity = 1.17. Conditions: [PBMA−Cl]/[$CuCl_2$]/[TPMA] = 1/0.42/1.5, $[P]_0$ = 1 M, T = 170 °C, and 1 h of reaction time. [b]The mole fraction of the degraded polymer f (%) estimated by ^{1}H NMR as ([polymer signal between 3.5 and 4.07 ppm]$_f$/[polymer signal between 3.5 and 4.07 ppm]$_0$) relative to diethyl phthalate O−CH_2 protons (4.34 ppm, integration between 4.16 and 4.6 ppm) as the internal standard. Initial = 0.1255 and final = 0.0509, f (%) = 41%. [c]The percent distilled monomer v (%) is estimated by ^{1}H NMR as 1 − ([total monomer and polymer signal between 3.5 and 4.16 ppm]$_f$/[total monomer and polymer signal between 3.5 and 4.16 ppm]$_0$) relative to diethyl phthalate O−CH_2 protons (4.34 ppm, integration between 4.16 and 4.6 ppm) as the internal standard. Initial = 0.1289 and final = 0.0828, so v (%) = 36%. [d]Molecular weight and dispersity of the high molecular weight polymer by GPC relative to the linear PMMA standards in THF.

experiments conducted using specialized equipment; however, the yield and selectivity were higher than that achieved in the pyrolysis of PMMA using a similar benchtop setup at 400 °C. Chain equilibration experiments confirmed that the depolymerization reactions likely stopped due to the loss of CEF before [M] = $[M]_{eq}$, as the activation of the macroinitiator at the same [M] still led to depolymerization despite the monomer being present. Additionally, the trends in $M_{n,GPC}$ vs. f also support the loss of CEF because there was only a slight shift in molecular weight and broadening in dispersity. This warranted further investigation into the thermal instability and CEF of the PBMA−Cl macroinitiator at 170 °C.

Thermal Analysis of PBMA−Cl. The PBMA−Cl macroinitiator was incubated at 170 °C under N_2 gas, in bulk, to assess whether uncatalyzed degradation of the polymer was appreciable at this temperature. Each incubated sample was characterized by GPC, ^{1}H NMR, and FT-IR. GPC of incubated PBMA−Cl showed a gradual decrease in molecular weight and dispersity with incubation time (Table 4). The macroinitiator decreased from an initial $M_{n,GPC}$ = 8750 and $Đ$ = 1.17 to $M_{n,GPC}$ = 8160 and $Đ$ = 1.16 after 120 min of incubation (Figure 7).

Table 4. Properties of Incubated PBMA−Cl

incubation time (min)	f[a]	$M_{n,GPC}$[b]	$Đ$[b]	$T_{d,1\%}$[c]	$T_{d,5\%}$[c]	$T_{d,10\%}$[c]	$T_{d,50\%}$[c]
0	0	8750	1.17	203	289	303	329
5	0.0012	8830	1.17	n.d.	n.d.	n.d.	n.d.
30	0.0077	8760	1.16	n.d.	n.d.	n.d.	n.d.
60	0.02	8320	1.19	n.d.	n.d.	n.d.	n.d.
120	0.025	8160	1.16	233	259	270	310

[a]Fraction of the BMA monomer determined by integration of vinyl proton signals relative to O−CH_2 protons in the side chain by ^{1}H NMR. [b]Molecular weight and dispersity were determined by THF GPC relative to the linear PMMA standards. [c]Thermal decomposition temperatures in °C, given at 1, 5, 10, and 50 wt % mass loss by high-resolution TGA with a dynamic heating rate under a nitrogen atmosphere.

^{1}H NMR analysis showed greater structural differences at longer incubation times. ^{1}H NMR analysis show partial depolymerization of the polymer, as evidenced by the increases in vinyl peak intensity at 6.10 and 5.55 ppm, a triplet at 4.16 ppm corresponding to −OCH_2− protons in the monomer side chain, and a singlet at 1.95 ppm from the α-CH_3 protons of the BMA monomer with incubation time (Figure S15). Uncatalyzed degradation of the chain end led to 2% depolymerization in the bulk and less than 1% at higher dilution in experiment L_0 (Table 1).

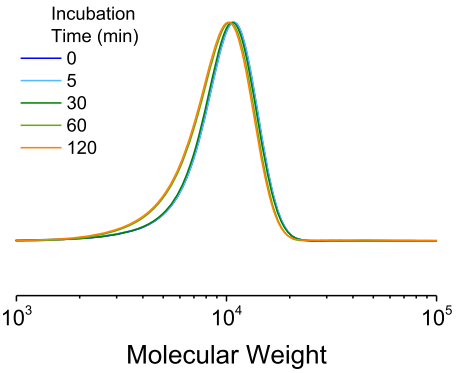

Figure 7. GPC of incubated PBMA−Cl. Molecular weight is given relative to the linear PMMA standards in THF.

There were no signs of chain-end elimination in the vinyl region. A high-intensity triplet at 3.55 ppm, corresponding to 1-chlorobutane, increased in intensity with incubation time (Figure S16). There was also a small amount of n-butanol present, as evidenced by the triplet at 3.65 ppm corresponding to the O−CH_2 protons of a n-butanol standard. FT-IR of the incubated PBMA−Cl macroinitiators revealed a new carbonyl absorbance band at 1780 cm^{-1} at long incubation times (Figures S17 and S18). The appearance of 1-chlorobutane, and the FT-IR absorbance at 1780 cm^{-1}, agrees with previous reports showing lactonization of halogen-capped methacrylates. The proposed mechanism of the lactonization reaction is given in Scheme S1. Incubation of bromine-functionalized alkyl methacrylate oligomers, prepared by telomerization with bromotrichloromethane or tetrabromomethane, produced oligomers with lactone chain ends with the same 1780 cm^{-1} absorbance after incubation.[47−50] The authors noted the appearance of alkyl bromines as byproducts after incubation of methyl methacrylate telomers with bromine functionality.[50] The same absorbance band was observed in the lactonization of PMMA−Cl and PMMA−Br after incubation in the bulk at 150 °C for half an hour.[51,52] The n-alkyl halide was detected as a volatile, and attributed to lactonization of the chain end, during the incubation of PMMA−Br prepared by ATRP using a 2,2,2-tribromoethanol initiator.[53]

Decomposition of end groups was also detected by high-resolution thermogravimetric analysis (HiRes-TGA) of the initial and incubated sample. HiRes-TGA of PBMA−Cl showed an additional step in thermal decomposition starting at a temperature of ∼150 °C, reaching a maximum rate of mass loss at 211 °C, before accelerated decomposition began at ∼290 °C (Figure S19). This led to a lower 1% thermal decomposition temperature ($T_{d,1\%}$) than the incubated macro-

https://doi.org/10.1021/acs.macromol.1c02246
Macromolecules 2022, 55, 78−87

Table 5. Chain Extensions and Blocking Efficiencies of Incubated Macroinitiators[a]

incubation time (min)	chain extension time (h)	conversion (%)[b]	$M_{n,th}$[b]	$M_{n,GPC}$[c]	$Đ$[c]	B[d]	ln (B/B_0)[e]
0	5	65	26,755	25,500	1.23	0.81	0
5	5	60	25,445	25,300	1.28	0.65	0.22
30	4.5	41	n.d.	n.d.	n.d.	n.d.	n.d.
	20	86	32,650	27,940	1.92	0.48	0.52
60	4.5	21	n.d.	n.d.	n.d.	n.d.	n.d.
	20	67	27,400	23,670	3.29	0.20	1.41
120	4.5	4	n.d.	n.d.	n.d.	n.d.	n.d.
	20	67	27,400	24,830	4.93	0.14	1.74

[a]Chain extension experiments were conducted using the mixture BMA/P(BMA)−Cl/$CuCl_2$/Me_6TREN = 200/1/1/1/1 at $[M]_0$ = 1.2 M and T = 90 °C with one-drop $Sn(EH)_2$. Total volume = 4 mL. [b]Theoretical molecular weight based on polymerization conversion by ^{1}H NMR. [c]Determined by THF GPC relative to the linear PMMA standards. [d]Initiation efficiency of the extended polymer determined by the multiple peak fitting of GPC traces (Supporting Information). [e]First-order logarithm for the change in initiation efficiency with incubation time.

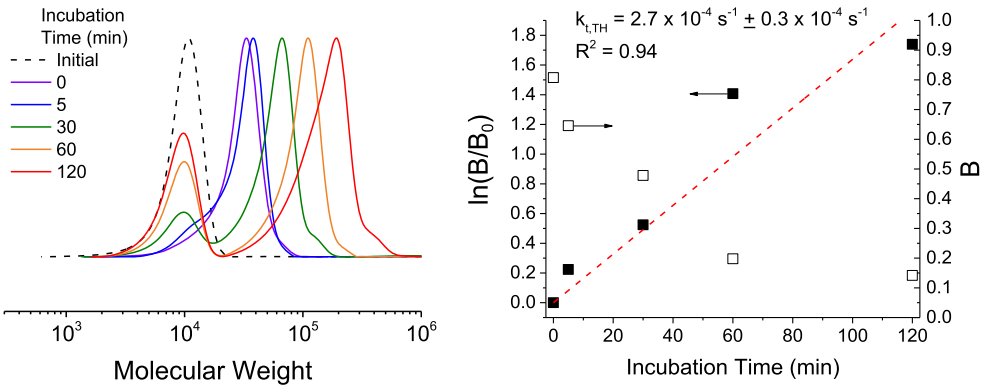

Figure 8. (Left) GPC traces of all chain extension experiments. The macroinitiator was incubated for a given amount of time at 170 °C before chain extension by AGET ATRP using a mixture of BMA/P(BMA)−Cl/$CuCl_2$/Me_6TREN = 200/1/1/1/1 at $[M]_0$ = 1.2 M and T = 90 °C with one drop of $Sn(EH)_2$ reducing agent. Total volume = 4 mL. (Right) first-order kinetic plot of decreasing blocking efficiency with incubation time. The slope of the line is an observed rate constant of thermal (uncatalyzed) loss of initiation efficiency with incubation time at 170 °C with a set y-intercept = 0. Blocking efficiencies were found by integration of the GPC traces normalized to the molecular weight scale.

initiator (Table 4). HiRes-TGA of the macroinitiator incubated for 2 h showed improved thermal stability at lower temperature, with the first stage of decomposition occurring at a much higher maximum of 269 °C but an overall poorer thermal stability than the macroinitiator at higher temperature (Figure S19). The lack of mass loss at low temperature in the incubated sample suggests that the first step in the thermal decomposition of PBMA−Cl occurs predominantly at the end groups. Incubation also improved the thermal stability of bromine-functionalized poly(n-alkyl methacrylate)s.[53] The opposite observation was observed in the TGA of P(PDMSMA)−Cl, which suggests that the side chains may influence the thermal stability of polymers prepared by ATRP.[43]

Loss of alkyl halide CEF was also observed in chain extension experiments of incubated macroinitiators as a decrease in initiation efficiency (Table 5). In this set of experiments, PBMA−Cl macroinitiators were incubated for a set amount of time at 170 °C, removed from the oil bath, and then dissolved in a stock solution of BMA/PBMA−Cl/$CuCl_2$/Me_6TREN = 200/1/1/1/1 at $[M]_0$ = 1.2 M. The chain extension experiments were started upon a one-drop injection of $Sn(EH)_2$. The initiation efficiency (B) of each chain extension was found by integration of the GPC traces after normalizing to a molecular weight scale (Figure S20). The non-normalized GPC traces in Figure 8 show a significant fraction of unreacted polymer, leading to bimodal molecular weight distributions, as the incubation time increased. The decrease in B with incubation time showed a relatively first-order kinetic behavior, with a rate constant of initiation efficiency loss of $k_{t,TH}$ = 2.7 × 10^{-4} s^{-1}. This corresponds to a "half-life" of alkyl chlorine initiation efficiency of 43 min at 170 °C.

CONCLUSIONS

The results of this article provide a comprehensive overview of the $CuCl_2$/TPMA-catalyzed and uncatalyzed degradation of a chlorine-capped poly(n-butyl methacrylate) (PBMA−Cl) macroinitiator prepared by ARGET ATRP. Catalyzed depolymerization proceeded via an ARGET mechanism using excess ligand as the reducing agent for both the $CuCl_2$/TPMA catalyst and the chlorine chain end. Depolymerization at $[P]_0$ = 0.75 M (8 wt % solids) with the complete $CuCl_2$/TPMA catalyst was rapid and recovered f (%) = 67% n-butyl methacrylate in 10 min. Catalyzed depolymerization reactions at higher solid loadings was faster but recovered less monomer, likely due to the decrease in $[M]_{eq,th}$ and an increase in radical concentration, leading to overall faster depolymerization to lower f.

The yields of all catalyzed depolymerization reactions at 170 °C were lower than those achieved by specialized pyrolysis reactors at temperatures ≥400 °C. Unlike depolymerization via pyrolysis, only chains containing chlorine functionality are available for depolymerization initiated via halogen abstraction. The low temperature of this setup improved the selectivity toward the monomer, as evidenced by the depolymerization

https://doi.org/10.1021/acs.macromol.1c02246
Macromolecules 2022, 55, 78−87

reactions on the rotary evaporator; however, loss of CEF accumulated kinetically trapped chains which could not be depolymerized under mild conditions. Thus, the reported depolymerization yields were justified by a non-quantitative 81% initiation efficiency for the macroinitiator, termination during the depolymerization process, and uncatalyzed degradation of the chlorine at the chain end.

Characterization of incubated macroinitiators by ^{1}H NMR and FT-IR agreed with the previous reports of lactonization of halogen-capped methacrylate oligomers at elevated temperature.[47−52] Loss of CEF was detected by high-resolution dynamic TGA measurements of the pristine PBMA−Cl macroinitiator as an additional step in mass loss beginning at 150 °C, leading to lower thermal stability. The initiation efficiency of chain extensions from incubated macroinitiators decreased with a half-lifetime of 43 min at 170 °C. It should be noted that poly(methyl methacrylate) with dithiobenzoate and trithiocarbonate functionalities are also prone to thermal decomposition within a temperature range of 120−180 °C.[54−56]

This study represents the catalyzed depolymerization of poly(methacrylates) via RDRP methods. The instability of chain ends and the lack of activation by other bond scission events away from the chain end emphasize the need for further investigation into catalyzed depolymerization methods, which maintain high livingness while avoiding thermal decomposition of inherently unstable chain ends. This presents a juxtaposition as higher temperatures favor depolymerization and also promote non-productive degradation routes which can stop the reaction. Catalyzed depolymerization at lower temperatures would follow "traditional" polymerization kinetics but would rely on judicious use of solvent due to the lower $[M]_{eq}$. The environmental impact of the solvent in space−time and energy efficiency will also need to be considered.

■ ASSOCIATED CONTENT

Supporting Information

The Supporting Information is available free of charge at https://pubs.acs.org/doi/10.1021/acs.macromol.1c02246.

Materials and instrumentation, synthetic procedures, ^{1}H NMR spectra, select crude ^{1}H NMR spectra, distillation/depolymerization experiments, GPC traces, and curve fitting analysis (PDF)

■ AUTHOR INFORMATION

Corresponding Author

Krzysztof Matyjaszewski − *Department of Chemistry, Carnegie Mellon University, Pittsburgh, Pennsylvania 15213, United States;* orcid.org/0000-0003-1960-3402; Email: matyjaszewski@cmu.edu

Authors

Michael R. Martinez − *Department of Chemistry, Carnegie Mellon University, Pittsburgh, Pennsylvania 15213, United States;* orcid.org/0000-0002-6211-763X

Ferdinando De Luca Bossa − *Department of Chemistry, Carnegie Mellon University, Pittsburgh, Pennsylvania 15213, United States*

Mateusz Olszewski − *Department of Chemistry, Carnegie Mellon University, Pittsburgh, Pennsylvania 15213, United States*

Complete contact information is available at: https://pubs.acs.org/10.1021/acs.macromol.1c02246

Notes

The authors declare no competing financial interest.

■ ACKNOWLEDGMENTS

We would like to acknowledge the financial support from NSF DMR 1921858 and NSF DMR 1501324. The NMR instrumentation at Carnegie Mellon University was partially supported by the NSF (CHE-0130903, CHE-1039870, and CHE-1726525). We thank S. Sydlik for generous access to the FT-IR instrument. We gratefully acknowledge Koei Chemical for providing the TPMA ligand used for all depolymerization experiments.

■ REFERENCES

(1) Braun, D. Origins and Development of Initiation of Free Radical Polymerization Processes. *Int. J. Polym. Sci.* **2009**, *2009*, 1−10.

(2) Pesenti, T.; Nicolas, J. 100th Anniversary of Macromolecular Science Viewpoint: Degradable Polymers from Radical Ring-Opening Polymerization: Latest Advances, New Directions, and Ongoing Challenges. *ACS Macro Lett.* **2020**, *9*, 1812−1835.

(3) Tardy, A.; Nicolas, J.; Gigmes, D.; Lefay, C.; Guillaneuf, Y. Radical Ring-Opening Polymerization: Scope, Limitations, and Application to (Bio)Degradable Materials. *Chem. Rev.* **2017**, *117*, 1319−1406.

(4) Yuan, J.; Wang, W.; Zhou, Z.; Niu, J. Cascade Reactions in Chain-Growth Polymerization. *Macromolecules* **2020**, *53*, 5655−5673.

(5) Yardley, R. E.; Kenaree, A. R.; Gillies, E. R. Triggering Depolymerization: Progress and Opportunities for Self-Immolative Polymers. *Macromolecules* **2019**, *52*, 6342−6360.

(6) Sagi, A.; Weinstain, R.; Karton, N.; Shabat, D. Self-Immolative Polymers. *J. Am. Chem. Soc.* **2008**, *130*, 5434−5435.

(7) Odian, G. *Principles of Polymerization*, 4; John Wiley & Sons, Inc., 2004.

(8) Dainton, F. S.; Ivin, K. J. Some Thermodynamic and Kinetic Aspects of Addition Polymerization. *Q. Rev., Chem. Soc.* **1958**, *12*, 61−92.

(9) Sawada, H. Chapter 3. Thermodynamics of Radical Polymerization. *J. Macromol. Sci., Polym. Rev.* **1969**, *3*, 357−386.

(10) Li, D.; Grady, M. C.; Hutchinson, R. A. High-Temperature Semibatch Free Radical Copolymerization of Butyl Methacrylate and Butyl Acrylate. *Ind. Eng. Chem. Res.* **2005**, *44*, 2506−2517.

(11) Wang, W.; Hutchinson, R. A.; Grady, M. C. Study of Butyl Methacrylate Depropagation Behavior Using Batch Experiments in Combination with Modeling. *Ind. Eng. Chem. Res.* **2009**, *48*, 4810−4816.

(12) Nasresfahani, A.; Hutchinson, R. A. Deterministic Approach to Estimate Functionality of Chains Produced by Radical Copolymerization in the Presence of Secondary Reactions. *Macromolecules* **2020**, *53*, 5674−5686.

(13) Li, D.; Li, N.; Hutchinson, R. A. High-Temperature Free Radical Copolymerization of Styrene and Butyl Methacrylate with Depropagation and Penultimate Kinetic Effects. *Macromolecules* **2006**, *39*, 4366−4373.

(14) Lahoud, I.; Balland, L.; Brodu, N.; Ben Talouba, I.; Mouhab, N.; Legrand, C. Thermokinetic parameters evaluation using reaction calorimetry: Application to butyl methacrylate solution radical polymerization. *Thermochim. Acta* **2020**, *691*, 178730.

(15) Tian, Q.; Zhao, H.; Simon, S. L. Kinetic study of alkyl methacrylate polymerization in nanoporous confinement over a broad temperature range. *Polymer* **2020**, *205*, 122868.

(16) Hutchinson, R. A.; Paquet, D. A.; Beuermann, S.; McMinn, J. H. Investigation of Methacrylate Free-Radical Depropagation Kinetics by Pulsed-Laser Polymerization. *Ind. Eng. Chem. Res.* **1998**, *37*, 3567−3574.

(17) Johnston, P. K.; Doyle, E.; Orzel, R. A. Acrylics: A Literature Review of Thermal Decomposition Products and Toxicity. *J. Am. Coll. Toxicol.* **1988**, *7*, 139−200.
(18) Kashiwagi, T.; Inaba, A.; Brown, J. E.; Hatada, K.; Kitayama, T.; Masuda, E. Effects of weak linkages on the thermal and oxidative degradation of poly(methyl methacrylates). *Macromolecules* **1986**, *19*, 2160−2168.
(19) Manring, L. E.; Sogah, D. Y.; Cohen, G. M. Thermal degradation of poly(methyl methacrylate). 3. Polymer with head-to-head linkages. *Macromolecules* **1989**, *22*, 4652−4654.
(20) Manring, L. E. Thermal degradation of poly(methyl methacrylate). 2. Vinyl-terminated polymer. *Macromolecules* **1989**, *22*, 2673−2677.
(21) Manring, L. E. Thermal Degradation of Poly(methyl methacrylate). 4. Random Side-Group Scission. *Macromolecules* **1991**, *24*, 3304−3309.
(22) Manring, L. E. Thermal degradation of saturated poly(methyl methacrylate). *Macromolecules* **1988**, *21*, 528−530.
(23) Moens, E. K. C.; De Smit, K.; Marien, Y. W.; Trigilio, A. D.; Van Steenberge, P. H. M.; Van Geem, K. M.; Dubois, J. L.; D'Hooge, D. Progress in Reaction Mechanisms and Reactor Technologies for Thermochemical Recycling of Poly(methyl methacrylate). *Polymers (Basel)* **2020**, *12*, 1667.
(24) Gilsdorf, R. A.; Nicki, M. A.; Chen, E. Y.-X. High chemical recyclability of vinyl lactone acrylic bioplastics. *Polym. Chem.* **2020**, *11*, 4942−4950.
(25) Grant, D. H.; Bywater, S. Thermal Depolymerization of Polymethylmethacrylate in Diphenylether Solution. *Trans. Faraday Soc.* **1963**, *59*, 2105−2112.
(26) Bywater, S.; Black, P. E. Thermal Depolymerization of Polymethyl Methacrylate and Poly-a-methylstyrene in Solution in Various Solvents. *J. Phys. Chem.* **1965**, *69*, 2967−2970.
(27) Kashiwagi, T.; Inabi, A.; Hamins, A. Behavior of primary radicals during thermal degradation of poly (methyl methacrylate). *Polym. Degrad. Stab.* **1989**, *26*, 161−184.
(28) Al-Salem, S. M.; Lettieri, P.; Baeyens, J. Recycling and recovery routes of plastic solid waste (PSW): a review. *Waste Manage.* **2009**, *29*, 2625−2643.
(29) Lehmann, F. A.; Brauer, G. M. Analysis of pyrolyzates of polystyrene and poly (methyl methacrylate) by gas chromatography. *Anal. Chem.* **1961**, *33*, 673−676.
(30) Kang, B.-S.; Kim, S. G.; Kim, J.-S. Thermal degradation of poly(methyl methacrylate) polymers: Kinetics and recovery of monomers using a fluidized bed reactor. *J. Anal. Appl. Pyrolysis* **2008**, *81*, 7−13.
(31) Vango, S. P.; Manatt, S. L. Quantitative pyrolysis gas chromatography of some acrylic copolymers and homopolymers. *Anal. Chem.* **1973**, *45*, 1251−1257.
(32) Awad, M. K. Effect of alkyl substituents on the thermal degradation of poly(alkyl methacrylate): a molecular orbital study using the ASED-MO method. *Polym. Degrad. Stab.* **1995**, *49*, 339−346.
(33) Bertini, F.; Audisio, G.; Zuev, V. V. Investigation on the thermal degradation of poly-n-alkyl acrylates and poly-n-alkyl methacrylates (C1−C12). *Polym. Degrad. Stab.* **2005**, *89*, 233−239.
(34) Czech, Z.; Pełech, R. Thermal degradation of poly(alkyl methacrylates). *J. Therm. Anal. Calorim.* **2010**, *101*, 309−313.
(35) Özlem, S.; Hacaloglu, J. Thermal degradation of poly(n-butyl methacrylate), poly(n-butyl acrylate) and poly(t-butyl acrylate). *J. Anal. Appl. Pyrolysis* **2013**, *104*, 161−169.
(36) Ettre, K.; Varadi, P. F. Pyrolysis-Gas Chromatographic Technique for Direct Analysis of Thermal Degradation Products of Polymers. *Anal. Chem.* **1962**, *34*, 752−757.
(37) Ettre, K.; Varadi, P. F. Pyrolysis-Gas Chromatographic Technique. Effect of Temperature on Thermal Degradation of Polymers. *Anal. Chem.* **1963**, *35*, 69−73.
(38) Ishitake, K.; Satoh, K.; Kamigaito, M.; Okamoto, Y. Stereogradient polymers formed by controlled/living radical polymerization of bulky methacrylate monomers. *Angew. Chem., Int. Ed. Engl.* **2009**, *48*, 1991−1994.
(39) Cho, H. Y.; Krys, P.; Szcześniak, K.; Schroeder, H.; Park, S.; Jurga, S.; Buback, M.; Matyjaszewski, K. Synthesis of Poly(OEOMA) Using Macromonomers via "Grafting-Through" ATRP. *Macromolecules* **2015**, *48*, 6385−6395.
(40) Martinez, M. R.; Cong, Y.; Sheiko, S. S.; Matyjaszewski, K. A Thermodynamic Roadmap for the Grafting-through Polymerization of PDMS11MA. *ACS Macro Lett.* **2020**, *9*, 1303−1309.
(41) Raus, V.; Čadová, E.; Starovoytova, L.; Janata, M. ATRP of POSS Monomers Revisited: Toward High-Molecular Weight Methacrylate−POSS (Co)Polymers. *Macromolecules* **2014**, *47*, 7311−7320.
(42) Flanders, M. J.; Gramlich, W. M. Reversible-addition fragmentation chain transfer (RAFT) mediated depolymerization of brush polymers. *Polym. Chem.* **2018**, *9*, 2328−2335.
(43) Martinez, M. R.; Dadashi-Silab, S.; Lorandi, F.; Zhao, Y.; Matyjaszewski, K. Depolymerization of P(PDMS11MA) Bottlebrushes via Atom Transfer Radical Polymerization with Activator Regeneration. *Macromolecules* **2021**, *54*, 5526−5538.
(44) Dong, H.; Matyjaszewski, K. ARGET ATRP of 2-(Dimethylamino)ethyl Methacrylate as an Intrinsic Reducing Agent. *Macromolecules* **2008**, *41*, 6868−6870.
(45) Sano, Y.; Konishi, T.; Sawamoto, M.; Ouchi, M. Controlled radical depolymerization of chlorine-capped PMMA via reversible activation of the terminal group by ruthenium catalyst. *Eur. Polym. J.* **2019**, *120*, 109181.
(46) Harrisson, S.; Mackenzie, S. R.; Haddleton, D. M. Pulsed Laser Polymerization in an Ionic Liquid:Strong Solvent Effects on Propagation and Termination of Methyl Methacrylate. *Macromolecules* **2003**, *36*, 5072−5075.
(47) Kimura, T.; Kodaira, T.; Hamashima, M. Separation and Structure of Methyl Methacrylate Telomers Synthesized in the Presence of Bromotrichloromethane. *Polym. J.* **1983**, *15*, 293−301.
(48) Kimura, T.; Hamashima, M. Study on Radical Telomerization of Esters of Methacrylic Acid by Using Bromotrichloromethane and Characteristics of the Resulting Telomers II. Primary Alkyl Methacrylates. *Polym. J.* **1986**, *18*, 21−30.
(49) Kimura, T.; Tasaka, H.; Hamashima, M. Study on Radical Telomerization of Esters of Methacrylic Acid Using Bromotrichloromethane and Characteristics of the Resulting Telomers IV. Branched Alkyl Methacrylates. *Polym. J.* **1987**, *19*, 305−314.
(50) Kimura, T.; Ezura, H.; Hamashima, M. Study on Telomerization of Methyl Methacrylate with Carbon Tetrabromide and Characteristics of the Resulting Adducts. *Polym. J.* **1992**, *24*, 187−197.
(51) Borman, C. D.; Jackson, A. T.; Bunn, A.; Cutter, A. L.; Irvine, D. J. Evidence for the low thermal stability of poly(methyl methacrylate) polymer produced by atom transfer radical polymerisation. *Polymer* **2000**, *41*, 6015−6020.
(52) Jackson, A. T.; Bunn, A.; Priestnall, I. M.; Borman, C. D.; Irvine, D. J. Molecular spectroscopic characterisation of poly(methyl methacrylate) generated by means of atom transfer radical polymerisation (ATRP). *Polymer* **2006**, *47*, 1044−1054.
(53) Camilo, A. P. R.; de Almeida, P.; Petzhold, C. L.; Felisberti, M. I. Thermal degradation of poly(alkyl methacrylate) synthesized via ATRP using 2,2,2-tribromoethanol as initiator. *Polym. Degrad. Stab.* **2018**, *158*, 1−13.
(54) Xu, J.; He, J.; Fan, D.; Tang, W.; Yang, Y. Thermal decomposition of dithioesters and its effect on RAFT polymerization. *Macromolecules* **2006**, *39*, 3753−3759.
(55) Chong, B.; Moad, G.; Rizzardo, E.; Skidmore, M.; Thang, S. H. Thermolysis of RAFT-synthesized poly (methyl methacrylate). *Aust. J. Chem.* **2006**, *59*, 755−762.
(56) Bekanova, M. Z.; Neumolotov, N. K.; Jablanović, A. D.; Plutalova, A. V.; Chernikova, E. V.; Kudryavtsev, Y. V. Thermal stability of RAFT-based poly(methyl methacrylate): A kinetic study of the dithiobenzoate and trithiocarbonate end-group effect. *Polym. Degrad. Stab.* **2019**, *164*, 18−27.

https://doi.org/10.1021/acs.macromol.1c02246
Macromolecules 2022, 55, 78−87